



## Gas sensing properties of Y-doped ZnO nanosheets synthesized via combustion method

Yan LI, Min LIU

Institute of Aerochemistry, College of Science, Civil Aviation University of China, Tianjin 300300, China

Received 9 September 2014; accepted 29 December 2014

**Abstract:** ZnO nanosheets doped with yttrium (Y) were synthesized via a solution combustion method using zinc nitrate and tartaric acid as raw materials. The scanning electron microscopy and X-ray powder diffraction were used to characterize ZnO nanosheets and the gas sensing properties of them were investigated. The results show that the as-synthesized ZnO nanosheets with diameters of 20–100 nm have a wurtzite structure with rough surface. The sensor made from the 2% Y-doped ZnO nanosheets exhibits a stronger response toward  $100 \times 10^{-6}$  (volume fraction) ethanol, its sensitivity at 300 °C is 17.50, and its optimal operating temperature (300 °C) is lower than that of the pure ZnO (330 °C). The obvious sensitivity (about 2.5) can be observed at the volume fraction of ethanol as low as  $5 \times 10^{-6}$ , while its the response time is only 2 s at 300 °C. Moreover, the Y-doped ZnO sensor has a better selectivity to ethanol than other gases.

**Key words:** ZnO; ethanol; Y-doping; combustion method; gas sensitivity

### 1 Introduction

Recently, as a highly promising II–VI semi-conducting metal oxide material with a wide direct band gap (3.37 eV) and high exciton binding energy (60 MeV), ZnO has attracted much attention for broad applications because of its advantageous features such as photoluminescence property, antibacterial activity, catalytic and high response to various toxic and pollutant gases [1,2]. Although, research on pure ZnO in the gas sensor field has a relatively long history, low sensitivity, long response time and poor selectivity have still limited its practical applications. Therefore, several effective technologies have been employed to enhance sensing properties such as adding catalysts or doping with other elements [3–7]. Many efforts have been devoted to improving the surface morphology, gas sensing, and luminescence properties by using the lanthanide-doping, such as La, Ce, Y and other elements [8–12]. WRIGHT et al [13] found that the catalyst metal coatings on GaN, InN and ZnO nanowires could obviously enhance the detection sensitivity for hydrogen gas sensing, but the

rates of response and recovery were relatively slow. NECMETTIN et al [14] harvested Y-doped ZnO thin films deposited on glass substrates by using sol–gel dip coating method with so much improved electrical property. YU et al [15] synthesized pure and Y-doped (1%, 3% and 7%, mole fraction) ZnO nanorods using a hydrothermal method. The gas sensing measurements showed that response and recovery time of 1% Y-doped ZnO nanorods-based sensor to  $100 \times 10^{-6}$  (volume fraction) acetone is about 30 s and 90 s at operating temperature of 400 °C, respectively. There is no doubt that doping Y strongly improved gas sensing ability, while the long-time response and high working temperature maybe limit the practical application of the material. It is a new challenge for Y as a dopant to decrease the operating temperature and speed up the response rate.

In this work, we focused on the synthesis and gas sensing properties of pure and Y-doped ZnO nanosheets with good ethanol sensing property using a simple modified solution combustion method. The as-prepared Y-doped ZnO exhibits high sensitivity (17.50 to  $100 \times 10^{-6}$  ethanol) and fast response (only 2 s to  $5 \times 10^{-6}$

**Foundation item:** Project (61079010) supported by the National Natural Science Foundation of China; Project (3122013P001) supported by the Significant Pre-research Funds of Civil Aviation University of China; Project (MHRD20140209) supported by the Science and Technology Innovation Guide Funds of Civil Aviation Administration of China

**Corresponding author:** Yan LI; Tel/Fax: +86-22-24092514; E-mail: liyan01898@163.com

DOI: 10.1016/S1003-6326(15)63837-7

ethanol) at 300 °C.

## 2 Experimental

### 2.1 Materials and apparatuses

All reagents of zinc nitrate ( $\text{Zn}(\text{NO}_3)_2 \cdot 6\text{H}_2\text{O}$ , AR,  $\geq 99.9\%$ ), tartaric acid ( $\text{C}_4\text{H}_6\text{O}_6$ , AR,  $\geq 99.7\%$ ), yttrium chloride ( $\text{YCl}_3 \cdot 6\text{H}_2\text{O}$ , AR,  $\geq 99.7\%$ ) and ethanol ( $\text{C}_2\text{H}_5\text{OH}$ , AR,  $\geq 99.7\%$ ) were commercially purchased, without any further purification.

X-ray diffraction (XRD) analysis was carried out with a DX-2000 diffractometer (Dandong Fang-Yuan Instrument Co., Ltd.) operated at 40 kV and 25 mA using Cu  $K_\alpha$  ( $\lambda=0.154184$  nm) radiation source employing a scanning rate of 0.05 ( $^\circ$ )/s with  $2\theta$  ranging from 30 $^\circ$  to 70 $^\circ$ . Field emission scanning electron microscope (FESEM, Hitachi X-650) was used to investigate the morphology of the samples.

### 2.2 Synthesis of Y-ZnO nanosheets

The Y-ZnO hybrid composites were prepared by a solution combustion method and the mole fractions of Y were 0, 1%, 2% and 4% by controlling the amount of  $\text{YCl}_3 \cdot 6\text{H}_2\text{O}$ . First of all, 2.975 g  $\text{Zn}(\text{NO}_3)_2 \cdot 6\text{H}_2\text{O}$  and 4.5 g  $\text{C}_4\text{H}_6\text{O}_6$  were completely dissolved in 30 mL deionized water, then, suitable amount of  $\text{YCl}_3 \cdot 6\text{H}_2\text{O}$  was added into the above homogeneous mixed solution. After continuous magnetic stirring for 30 min, the precursor solution was transferred into an electric furnace for heating a period of time until the samples became fine grains. Then, the system is heated up to 500 °C, kept this temperature for 1 h, and cooled down to room temperature naturally. The products were harvested after washing the precipitates completely with deionized water and ethanol several times and finally dried at 60 °C in air for further characterizations.

### 2.3 Fabrication and measurement of sensors

Y-doped ZnO powders were mixed with proper distilled water and ground in an agate mortar for a while to obtain an oxide paste. The as-prepared paste was coated on the outer surface of the cleaned alumina tube on which a pair of Pt electrodes was connected already to form the sensor. Then, the fabricated gas sensors were installed on the sensor aging equipment at 80 mA for 48 h before measurement in order to attain stable electrical resistance values. The gas sensing measurements were performed on a chemical gas sensor-8 intelligent analysis system (Beijing Elite Tech Co., Ltd., China) and the operating temperature of the static system was controlled from 180 °C to 390 °C by changing the heating current. The gas sensing sensitivity ( $S$ ) is defined as the ratio ( $R_a/R_g$ ) of the electrical resistance of the sensor in the air ( $R_a$ ) to that of the target

gas ( $R_g$ ). The response (or recovery) time is the time taken by the sensor to achieve 90% of the equilibrium value in the case of adsorption (or desorption).

## 3 Results and discussion

### 3.1 XRD analysis

Figure 1 shows the typical XRD patterns of the as-synthesized pristine ZnO doped with different mole fractions of Y being 0, 1%, 2% and 4%, respectively. All of the intense ZnO Bragg reflections of pristine ZnO can be perfectly assigned to those of hexagonal phase ZnO (JCPDS card No. 36-1451) with lattice parameters  $a$  and  $c$  of 0.3251 nm and 0.5207 nm, respectively, which confirms crystalline ZnO nanostructures exhibiting a wurtzite structure. The samples prepared in this work are of high purity and crystallinity because of the sharp diffraction peaks and no other characteristic peaks from any impurities. Being modified with increasing content of Y, the diffraction peaks at  $2\theta$  of 36.5 $^\circ$  became weak and slightly shifted to the light direction. This implied that the lattice space became small but increased, maybe due to Zn vacancy occurring while a few Y atoms replaced Zn atoms.

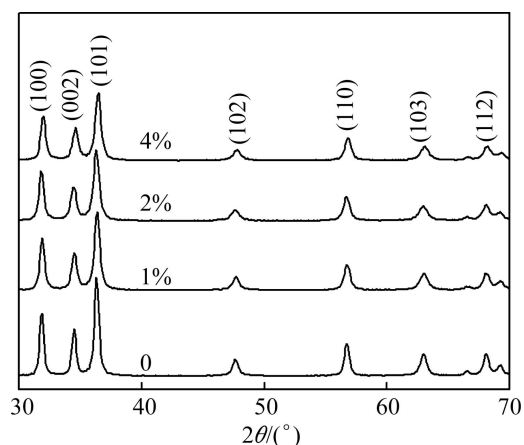


**Fig. 1** XRD patterns of Y-ZnO nanosheets doped with different Y contents of 0, 1%, 2% and 4%

### 3.2 FESEM investigation

The morphologies of Y-ZnO nanosheets doped with Y mole fractions of 0, 1%, 2% and 4% are shown in Figs. 2(a) and (b). As seen in Fig. 2(a), the four samples have a rough external surface and exhibit homogeneous nanosheets aggregated with a diameter of 20–100 nm approximately. Although no obvious differences of their profile and grain size are observed, the surface morphology and the packing density of the above samples change after Y doping. For the 2% Y-doped ZnO sample, the grain size is almost the same and the nanosheets are more uniformly distributed over the whole sample surfaces. The low magnified image in

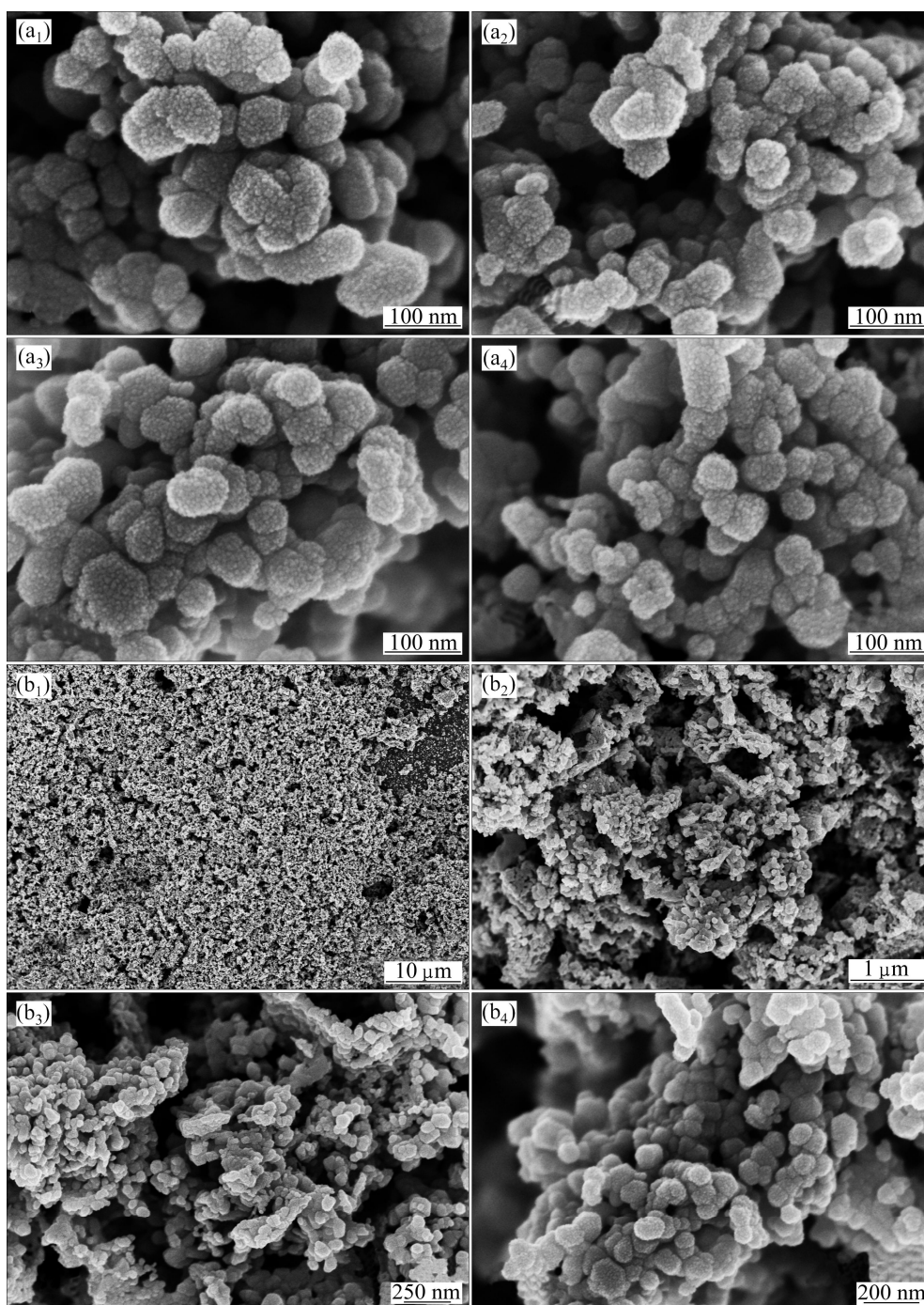


**Fig. 2** SEM images of Y-ZnO nanosheets doped with Y mole fractions of 0 (a<sub>1</sub>), 1% (a<sub>2</sub>), 2% (a<sub>3</sub>), and 4% (a<sub>4</sub>) at same magnification and morphologies of 2% Y-doped ZnO (b<sub>1</sub>, b<sub>2</sub>, b<sub>3</sub>, b<sub>4</sub>)

Fig. 2(b<sub>1</sub>) shows the overview of the regular ZnO nanosheets, from which a uniform structure can be clearly observed. In the higher magnification micrograph (Fig. 2(b<sub>4</sub>)), we can find large gap among the nanosheets when they gather together, which contributes to their gas sensing properties.

### 3.3 Gas-sensing properties

The operating temperature-dependent sensing

behaviors of the pure and Y-doped ZnO nanosheet sensors from 180 to 390 °C at a step of 30 °C exposed to  $100 \times 10^{-6}$  (volume fraction) ethanol were investigated and shown in Fig. 3. It is noteworthy that the response values for each sample are found to increase slowly with increasing temperature at first while decrease dramatically with a further rise of the operating temperature. While Y-doped ZnO samples exhibit the highest sensitivity of 17.50, the sensitivity of undoped

ZnO nanostructure is only 5.63 at 300 °C. Furthermore, the optimal operating temperature of the 2% Y-doped ZnO nanosheet sensor (300 °C) is lower than that of the pure ZnO (330 °C) and the corresponding sensitivity is much higher. The fact that 2% Y-doped ZnO exhibits the highest sensitivity can be explained from the kinetics and mechanics of fast gas adsorption and desorption on the surface of the sample at the maximum response temperature. For further comparison and evaluation, 300 °C was selected to be the optimum operating temperature for gas sensing with ZnO and Y-doped ZnO sensor and was applied to other sensing property tests afterward.

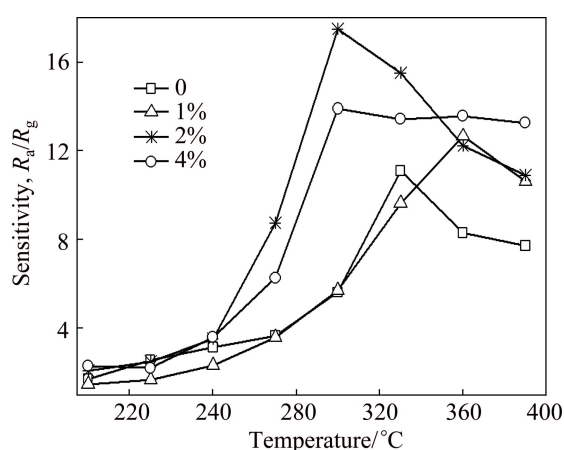


**Fig. 3** Sensitivities of Y-ZnO nanosheets doped with different mole fractions of Y to  $100 \times 10^{-6}$  ethanol at different temperatures

Figure 4 shows the sensor responses of 0, 1% Y, 2% Y, and 4% Y-doped ZnO nanosheet gas sensors versus different volume fractions of ethanol vapor at 300 °C. It can be seen that the sensitivity of all investigated sensors linearly increases with increasing the volume fraction of ethanol vapor without showing any saturation. And the sensitivity of sensor based on 2% Y-doped ZnO nanosheets is superior to that based on other ZnO

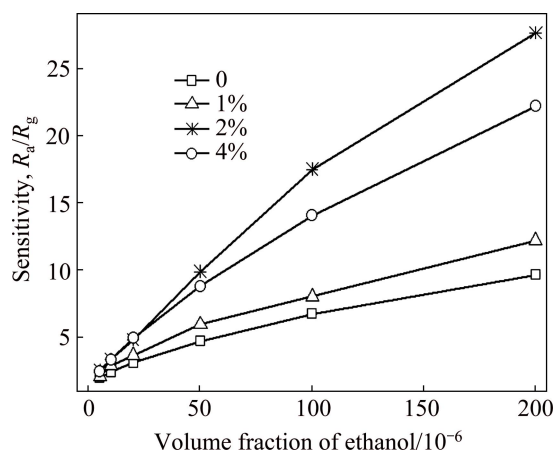


**Fig. 4** Sensitivities of Y-ZnO nanosheets doped with different

Y contents versus volume fraction of ethanol gas at 300 °C nanosheets for each concentration in all the measurements. For example, the sensitivity of the 2% Y-doped ZnO sensor to  $200 \times 10^{-6}$  ethanol at 300 °C reaches 27.65, which is about 3 times that of pure ZnO sample (just 9.66). Moreover, the high sensitivity of these sensors can also be observed upon exposure to ethanol content as low as  $5 \times 10^{-6}$  (the corresponding sensitivities are about 2.5), indicating that these special structures may be a kind of promising ethanol sensor material.

Figure 5 represents the dynamic sensitivity variation of ZnO and 2% Y-ZnO based sensors toward  $5 \times 10^{-6}$  ethanol at 300 °C. As shown in Fig. 5, when the environment is switched from air to ethanol vapor, the sensitivities of both sensors increase rapidly, indicating that Y doping maintains the n-type semiconducting properties of pristine ZnO. Furthermore, the response time of the 2% Y-ZnO nanosheet-based sensor is 2 s to  $5 \times 10^{-6}$  ethanol, which is much shorter than that of pure ZnO (4 s), revealing that high and fast gas response ZnO nanostructure sensing material can be achieved after Y-doping.

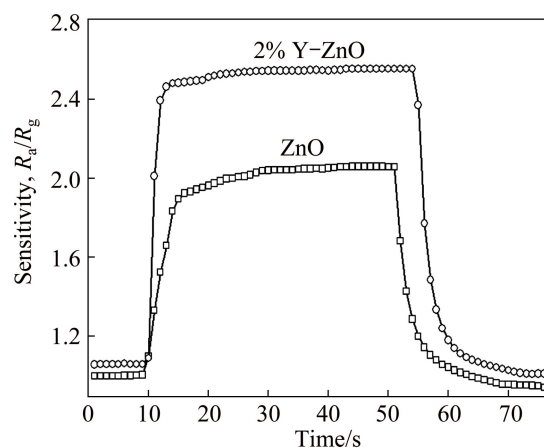


**Fig. 5** Response and recovery characteristics of ZnO and 2% Y-ZnO to  $5 \times 10^{-6}$  ethanol at 300 °C

The gas-sensing selectivities of the sensors were investigated by exposing the response to  $100 \times 10^{-6}$  various gases, including benzene ( $C_6H_6$ ), formaldehyde (HCHO),  $H_2$ , acetone ( $C_3H_6O$ ), ethanol ( $C_2H_5OH$ ), CO and  $CH_4$  at 300 °C, as shown in Fig. 6(a). Apparently, the responses of Y-ZnO to ethanol vapor are markedly higher than those to the investigated interference gases. The sensitivity of 2% Y-ZnO-based sensor is about 17.5 to ethanol, while the highest sensitivity to other gases is 6.56, the great sensitivity contrast of ethanol to other test gases means that Y-doped ZnO has very good selectivity. The stability of the 2% Y-ZnO-based sensor was investigated for four switching times by cycling through dry air to ethanol gas and back to dry air processes in a

similar manner to that of previous measurements, as shown in Fig. 6(b). After four cycles, no significant sensitivity degradation was found, confirming a good reproducibility of the sensor.

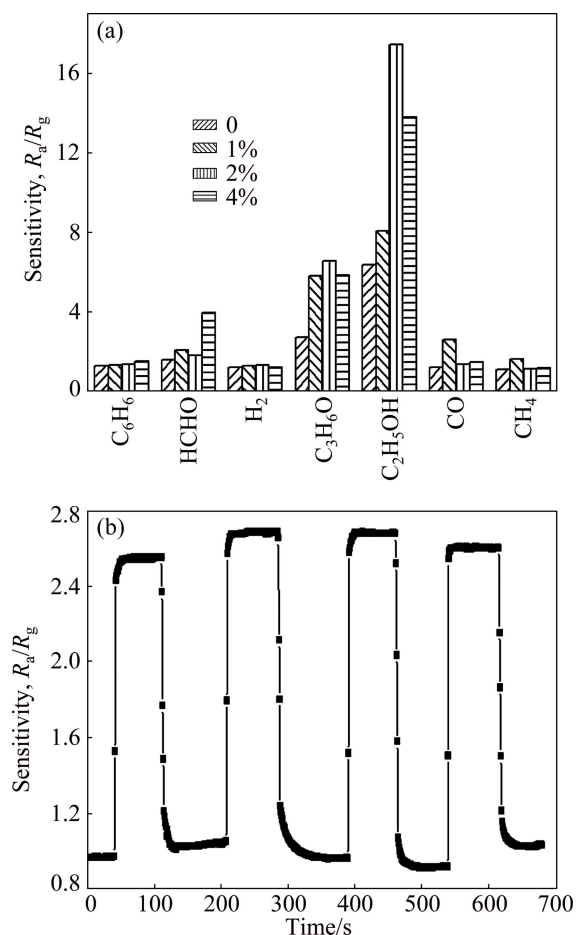
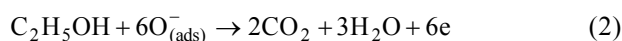


**Fig. 6** Selectivity histogram of Y–ZnO with Y mole fractions of 0, 1%, 2%, and 4% towards  $100 \times 10^{-6}$  of different gases at 300 °C (a) and sensitivity of pure ZnO to  $5 \times 10^{-6}$  ethanol at 300 °C (b)

The sensing mechanism of the Y–ZnO nanosheets to reducing gases (such as ethanol) may be explained as follows: being a surface-controlled type sensor, the rate of response is influenced seriously by many factors such as the grain size and surface defects. When exposed to air, the oxygen molecules are chemisorbed on the ZnO surface by acquiring electrons from the conduction band of the semiconductor and forming ionic species ( $O_{(ads)}^-$ ), hence increasing the resistance because of the formation of depletion layers on the surface of ZnO nanosheets. Free electrons (e) are released quickly when ethanol is added, and then injected into the conduction band of the ZnO, thereby decreasing the resistance and increasing the sensitivity. The reactions include



Although the microstructural characterization (crystallite size and shape) gave no indication of the formation of ZnO structures with different Y loadings, obvious increase in the electrical resistance illustrated that Y may enter the lattice structure of zinc oxide [16]. The component Y segregating into a separate phase to form a new energy band can sharply decrease the necessary energy for the desorption reaction. Additionally, the observed faster reaction kinetics may be also due to the catalytic role of Y in imparting the sensor response through electronic sensitization mechanism via providing a higher density of active sites by the additives. The Y dopant not only activates the reaction between surface oxygen and ethanol molecules, but also reduces the adsorption of reacting molecules.

## 4 Conclusions

1) Y-doped ZnO nanosheets with diameters of 20–100 nm and a rough surface were prepared via a solution combustion method using zinc nitrate and tartaric acid as raw materials.

2) The sensor made from the 2% Y-doped ZnO nanosheets exhibits a stronger response to  $5 \times 10^{-6}$  ethanol as high as 2.5, while the response time is only 2 s at 300 °C.

3) The sensitivity of the 2% Y–ZnO-based sensor is about 17.5 to  $100 \times 10^{-6}$  ethanol, while the highest sensitivity to other gases is 6.56. The great sensitivity contrast of ethanol to other test gases means that Y-doped ZnO has very good selectivity.

4) The cycle-test of the 2% Y–ZnO-based sensor shows that no significant sensitivity degradation confirms a good reproducibility of the sensor.

## References

- [1] SHINDE S D, ATIL G E, KAJALE D D, GAIKWAD V B, JAIN G H. Synthesis of ZnO nanorods by spray pyrolysis for  $H_2S$  gas sensor [J]. *Journal of Alloys and Compounds*, 2012, 528: 109–114.
- [2] LI Yan, LI Guo-zhu, ZOU Yun-ling, WANG Qiong, ZHOU Qing-jun, LIAN Xiao-xue. Preparation and sensing performance of petal-like  $RuO_2$  modified ZnO nanosheets via a facile solvothermal and calcination method [J]. *Transactions of Nonferrous Metals Society of China*, 2014, 24(9): 2896–2903.
- [3] WEI S H, YU Y, ZHOU M H. CO gas sensing of Pd-doped ZnO nanofibers synthesized by electrospinning method [J]. *Materials Letters*, 2010, 64: 2284–2286.
- [4] CHOI S W, KIM S S. Room temperature CO sensing of selectively grown networked ZnO nanowires by Pd nanodot functionalization [J]. *Sensors and Actuators B: Chemical*, 2012, 168: 8–13.
- [5] YU C L, YANG K, ZHOU W Q, FAN Q Z, WEI L F, YU J C. Preparation, characterization and photocatalytic performance of noble metals (Ag, Pd, Pt, Rh) deposited on sponge-like ZnO microcuboids [J]. *Journal of Physics and Chemistry of Solids*, 2013, 74: 1714–1720.

- [6] ZHANG S Y, CAO Q X. First-principles and experimental studies of the IR emissivity of Sn-doped ZnO [J]. *Materials Science in Semiconductor Processing*, 2013, 16: 1447–1453.
- [7] HUANG F C, CHEN Y Y, WU T T. A room temperature surface acoustic wave sensor with Pt coated ZnO nanorods [J]. *Nanotechnology*, 2009, 20: 065501–065506.
- [8] CHANG C J, LIN C Y, CHEN J K, HSU M H. Ce-doped ZnO nanorods based low operation temperature NO<sub>2</sub> gas sensors [J]. *Ceramics International*, 2014, 40: 10867–10875.
- [9] RASHID T R, PHAN D T, CHUNG G S. Effect of Ga-modified layer on flexible hydrogen sensor using ZnO nanorods decorated by Pd catalysts [J]. *Sensors and Actuators B: Chemical*, 2014, 193: 869–876.
- [10] MANSOOR A, SEYYED E M F. Humidity sensing properties of Ce-doped nanoporous ZnO thin film prepared by sol–gel method [J]. *Journal of Rare Earths*, 2012, 30: 38–42.
- [11] HE J Q, YIN J, LIU D, ZHANG L X, CAI F S, BIE L J. Enhanced acetone gas-sensing performance of La<sub>2</sub>O<sub>3</sub>-doped flowerlike ZnO structure composed of nanorods [J]. *Sensors and Actuators B: Chemical*, 2013, 182: 170–175.
- [12] LI X B, ZHANG Q Q, MA S Y, WAN G X, LI F M, XU X L. Microstructure optimization and gas sensing improvement of ZnO spherical structure through yttrium doping [J]. *Sensors and Actuators B: Chemical*, 2014, 195: 526–533.
- [13] WRIGHT J S, WANTAE L, NORTON D P, PEARTON S J, REN F, JASON L J, ANT U. Nitride and oxide semiconductor nanostructured hydrogen gas sensors [J]. *Semiconductor Science and Technology*, 2010, 25: 024002–024009.
- [14] NECMETTIN K, SADULLAH O, LUTFI A, AHMET A, ZAFER Z O. Structural, electrical transport and NO<sub>2</sub> sensing properties of Y-doped ZnO thin films [J]. *Journal of Alloys and Compounds*, 2012, 536: 138–144.
- [15] YU P, WANG J, DU H Y, YAO P J, HAO Y W, LI X G. Y-doped ZnO nanorods by hydrothermal method and their acetone gas sensitivity [J]. *Journal of Nanomaterials*, 2013, 2013: 751826: 1–6.
- [16] HJIRI M, MIR L E, LEONARDI S G, PISTONE A, MAVILIA L, NERI G. Al-doped ZnO for highly sensitive CO gas sensors [J]. *Sensors and Actuators B: Chemical*, 2014, 196: 413–420.

## 燃烧法制备的 Y 掺杂 ZnO 纳米片的气敏性能

李 酏, 刘 敏

中国民航大学 理学院 航空化学研究所, 天津 300300

**摘 要:** 以硝酸锌和酒石酸为原料, 采用液体燃烧法制备钇(Y)掺杂的氧化锌纳米片。利用 XRD 和 SEM 对其微观结构进行表征, 并研究 Y 掺杂量对 ZnO 气敏性能的影响。结果表明: 所制备的 ZnO 为纤锌矿结构且表面粗糙, 呈纳米片状, 直径为 20~100 nm。以 Y 掺杂量为 2%(摩尔分数)的氧化锌制成的传感器在 300 °C 时对体积分数为  $100 \times 10^{-6}$  的乙醇的灵敏度高达 17.50, 其最佳工作温度(300 °C)低于未掺杂 ZnO(330 °C)。当乙醇气体的体积分数低至  $5 \times 10^{-6}$  时, ZnO 传感器也有明显的灵敏度值(约为 2.5), 且在 300 °C 工作时响应时间仅为 2 s。相比于其他气体, 该种传感器对乙醇表现出极好的选择性。

**关键词:** ZnO; 乙醇; Y 掺杂; 燃烧法; 气敏性能

(Edited by Wei-ping CHEN)